MEASUREMENT OF THE ADHESION ENERGY IN A Cu-C INTERFACE

D. Marcos-Gómez[1], J. Tamayo-Ariztondo[1], J. Garagorri[1] D. González[1], J.M. Molina-Aldareguia[2], M.R. Elizalde[1]

[1] CEIT and TECNUN (University of Navarra). Manuel de Lardizábal 15, 20018 San Sebastián, Spain
E-mail: dmarcos@ceit.es

[2]Fundación IMDEA-Materiales, c/Profesor Aranguren s/n, 28040 Madrid, Spain

ABSTRACT

Recently, Cu/C composites have been developed for heat sink applications. Yet, it is known that the adhesion between copper and carbon is weak due to its poor wetting [1]. To improve interfacial properties, Cr or Ti interlayers are used so that the adhesion between Cu and C enhances considerably. In order to measure adhesion in terms of energy, Cu-C flat systems have been prepared. These systems consist of an amorphous carbon substrate with a Cu coating, either with or without a Ti interlayer. Top nanoindentation is performed with a Berkovich tip nanoindenter which penetrates the top surface of the sample, i.e., the coating, and causes debonding of the interface if the driving force introduced by the indentation exceeds the interfacial bond strength. The crack formed in the debonding enables to measure the adhesion energy through an equation derived from the mechanical analysis on layered systems by Marshall and Evans [2].

These experimental results are used to calibrate a cohesive law for a model based on finite elements. The parameters peak stress, maximum equivalent displacement, initial stiffness and adhesion energy of the cohesive law, three of which are independent, have to be determined to this end. Results from the analytical and numerical model are compared. The fact that Marshall-Evans formula does not take into account the plastic energy dissipated by the Cu layer to calculate the fracture energy of the interface from top indentation tests is also discussed.

KEY WORDS: Cu/C composite, adhesion energy, cohesive elements, FEM, nanoindentation

INTRODUCTION

Copper-Carbon Nanofiber (Cu-CNF) composite materials have very promising theoretical properties, specifically, when considering thermal and electrical conductivities. Unfortunately, Cu and CNF show a very weak adhesion as the wetting between them is very poor [1]. This can be solved with interfacial nanometric layers of elements like Ti or Cr. In order to assess the interfacial toughness improvement achieved top nanoindentation tests have been performed on a flat system. This system consists of a Cu layer on top of an amorphous carbon substrate with or without a Ti interlayer. With the data obtained in these experiments, the fracture energy of the interface can be calculated through the equation of Marshall and Evans [2].

Cohesive elements are a very powerful tool to analyse fracture in adhesive layers or in interfaces (for example [3]), but due to their phenomenological nature they demand to be calibrated through experimental data in order to offer realistic results. In addition, some properties of the materials under study may be not entirely or accurately known, which allows for parametric studies of the indentation process, that include other parameters apart from those defining the cohesive elements. Once these are calibrated, complex models of finite elements can be built placing these in the interface between phases, which is the part of the composite prone to fracture, especially for weak interfaces.

EXPERIMENTAL PROCEDURE

The samples tested for mechanical adhesion consist of a 3 μm thick Cu thin film sputtered by Physical Vapour Deposition (PVD) onto a 10 x 10 x 1.5 mm amorphous carbon substrate. In addition, one of the samples contains a very thin (2.5 nm) interlayer of titanium. The notation and description of the samples are shown in table 1.

Table 1. Samples tested with their notation and principal characteristics.

Notation	Interlayer (thickness)	Thickness of Cu layer
17.1	None	3000 nm
17.2	Ti (2.5 nm)	3000 nm

Residual stress analysis

Prior to indentation, residual stresses of the Cu thin films have been measured by the parallel beam glancing X-ray diffraction technique [4]. The diffractometer used

in this work is a Philips X'Pert MRD, which was operated at a voltage of 40 kV and a current of 40 mA. A Cu tube was used to emit in the X-Ray wavelength $K_{\alpha 1}$ = 1.540562 Å [5].

Glancing is a useful method to characterise the spacing between planes in thin films, hence enables to quantify residual stresses in the film. It principally consists on irradiating the material at a very low incident angle with respect to its surface. This enables a very low penetration depth, hence avoiding any interaction with the substrate. The Glancing method was carried out with a linear primary optic. The apertures for the low angle slits at the primary optic were set as 10 for vertical slit and 1/16th for the horizontal slit. A value of ω = 3 º was determined for the incident angle. A solution of free stressed silicon crystals and 2-propanol (isopropyl alcohol) was spread over sample surfaces. The free stressed crystals permit to detect and estimate the errors principally introduced from absorption of the specimen and displacement of the specimen from the diffractometer axis, which is considered as the largest single source of error [6].

Top Nanoindentation tests

The Top Nanoindentation method consists in indenting the thin film on the top surface so that a crack at the interface between the film and the substrate appears [7-9]. The apparatus used in this work to attempt interface debonding on samples 17.1 and 17.2 is a NanoIndenter® II (Agilent, formerly Nano Instruments, Inc.). The indentation tip used for the experiments is a Berkovich tip, a three-sided diamond pyramid. All the indentation tests were carried out under displacement control at a maximum penetration depth varying from 400 nm to 2500 nm.

Adhesion energy was calculated using the Marshall & Evans equation (ME) [2]:

$$G = \frac{h\sigma_I{}^2(1-\nu^2)}{2E} + (1-\alpha)\frac{h\sigma_R{}^2(1-\nu)}{E} - (1-\alpha)\frac{h(\sigma_I-\sigma_B)^2(1-\nu)}{E} \quad (1)$$

where h is the coating thickness, E and ν are the Young's modulus and Poisson's ratio of the coating (110 GPa and 0.343), respectively, and α is a parameter equal to 1 - 1/(1 + 0.902(1 - ν)) when buckling has occurred and equal to 1 when no buckling has been observed. This equation considers the substrate as infinitely rigid, i.e., changes in its strain energy are negligible when the delamination radius is much larger than the film thickness. The film is considered to experience a biaxial stress field.

σ_I is the stress provoked by the indentation and is described as:

$$\sigma_I = \frac{EV_I}{2\pi h a^2(1-\nu)} \quad (2)$$

where V_I is the indented volume and a half of the crack length provoked by the delamination.

σ_R is the residual stress measured in the Cu thin film. If the driving force is sufficiently high, delamination can cause buckling of the Cu layer. The buckling condition is ruled by the critical biaxial buckling stress σ_B, given by [6]:

$$\sigma_B = \mu^2 \frac{h^2 E}{12a^2\left(1-\nu^2\right)} \quad (3)$$

where μ^2 is equal to 14.68 for single buckling and equal to 42.67 for annular buckling or centre-pinned clamped-clamped plate.

A FIB dual beam Quanta FEG 3D (FEI) was used to measure the crack length 2a produced during indentation, in order to calculate the adhesion energy G. A trench was milled across the indentations in order to achieve direct observation of the delamination occurred when indenting a Cu-C sample at different depths with a Berkovich tip.

FINITE ELEMENT MODEL

A finite element (FE) model was prepared using the FE commercial suite ABAQUS to reproduce the nanoindentation experiments. The model consisted in 60º slice of the actual specimen, as the Berkovich tip has mirror and three-fold rotational symmetry. The model is 40 μm high, including the 3 μm thick Cu layer adhered by a zero-thickness cohesive layer (i.e., a layer made of cohesive elements) to the remaining 37 μm of vitreous carbon. This cohesive layer was based on the phenomenological concept of cohesive zone that is used in FE modelling for fracture mechanics and was built with COH3D8 elements. A refined mesh was used around the indentation, both in the Cu and the carbon substrate, and around the expected crack.

Table 2. Elastic properties used to model copper and carbon.

	Young Modulus (GPa)	Poisson's Ratio
Copper [10]	110	0.343
Vitreous Carbon	26[11]	0.343

Table 2 shows the elastic properties of the two materials constituting the model. The substrate was defined as an elastic material in all the simulations so no energy is spent in plastic deformation of the substrate. Poisson's

ratio of the vitreous carbon was unknown and it was assumed to have the same value as for Cu which should not influence the final results. It is important to notice that Cu is four times stiffer than the vitreous carbon, which means that the substrate was noticeably affected by the indentations. Regarding the Cu film, it is modelled as an elastic-plastic material with strain hardening defined by the Hollomon's equation. The behaviour of thin films is a subject open to discussion so yield stress and the strain hardening coefficient are initially considered parameters to study its influence on the calculation of the interfacial fracture energy. Finally, according to experimental measurements, a tensile residual stress of 300 MPa is introduced in the Cu layer (table 3).

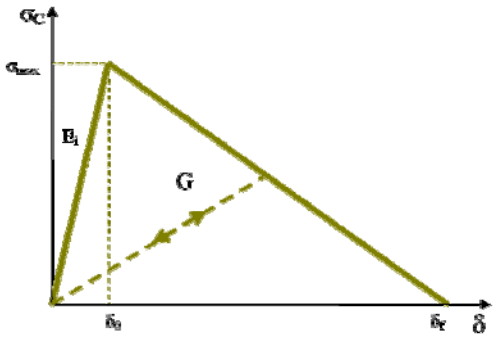

Figure 1. Scheme of the traction-separation law used in the cohesive elements. Four parameters, three of which are independent, define the triangular law: fracture energy (G), peak stress (σ_{max}), initial stiffness (E_i) and final displacement (δ_f),.

A triangular law is used to define the cohesive elements behaviour (fig. 1) [12]. This law is defined by four parameters of which only three are independent. Fracture energy (G), peak stress (σ_{max}) and initial stiffness (E_i) have been used as parameters to calibrate the cohesive law.

EXPERIMENTAL RESULTS

The structure of the Cu coating in samples 17.1 and 17.2 can be observed in figure 2. The effect of the 2.5 nm thick Ti interlayer is noticeable; whereas the sample without interlayer shows a Cu coating with high roughness and porosity, these effects are significantly reduced in the presence of the interlayer.

Figure 3 shows the evolution of crack radius with the penetration depth of the indentation in sample 17.2. It can be observed that the evolution of crack radius is linear with the maximum penetration depth during top indentation. Similar data could not be obtained for sample 17.1 since either no cracks at the interface were generated or the data were not consistent. This is due to the abovementioned roughness and porosity of the Cu coating which is probably related to the poor wetting between Cu and C. An example is shown in figure 4, where at low penetration depth the indenter only came into contact with a unique grain. Thus only data obtained at a penetration depth of 2500 nm have been considered for calculating interfacial fracture energy with ME equation [2]. The results are gathered in Table 3.

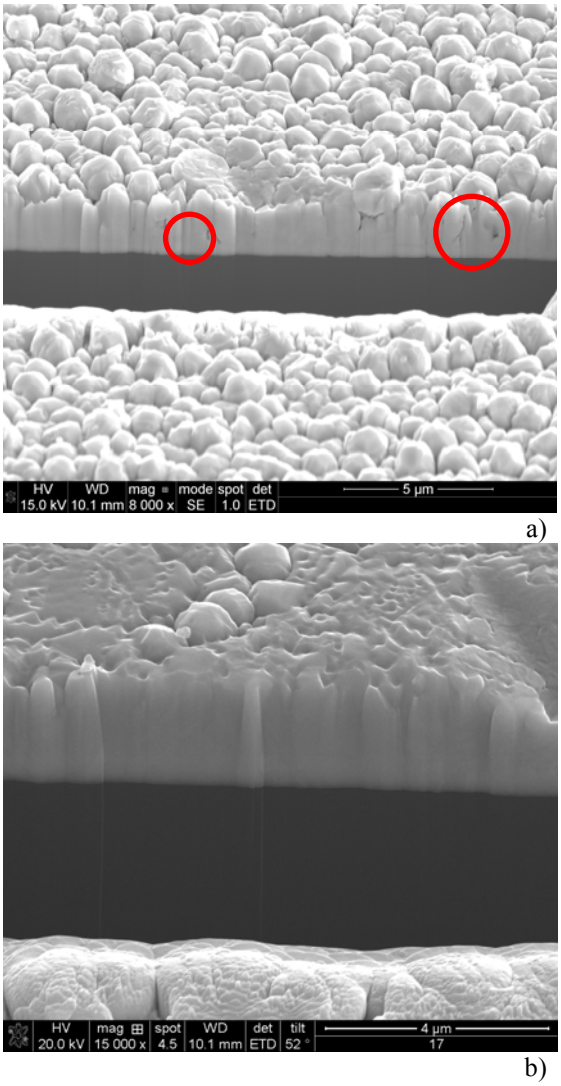

Figure 2. SEM pictures of a trench milled with the FIB on a) sample 17.1 and; b) sample 17.2. Some pores are highlighted with circles in sample 17.1.

Table 3. Average residual stresses, interfacial crack length after a top indentation tests performed at a maximum depth of 2500 nm and calculated adhesion energy using eq. (1) [2] for samples 17.1 and 17.2.

Sample	Residual Stress (MPa)	Adhesion Energy (J/m^2)	Crack Length (µm)
17.1	290 ± 40	24 ± 4	25 ± 1
17.2	307.10 ± 0.05	70 ± 30	19 ± 2

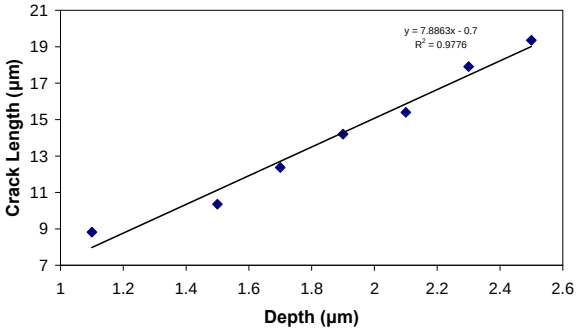

Figure 3. Crack radius against maximum penetration depth during top indentation. Sample 17.2.

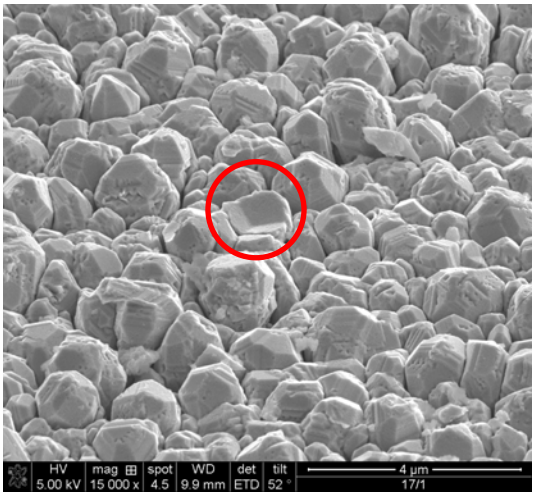

Figure 4. Imprint of a 400 nm depth indentation in a grain of sample 17.1 (circled).

Regarding the effect of the residual stresses in the Cu coating, it can be observed that they are tensile and similar for both samples and hence buckling has not occurred during top indentation tests.

Finally, a significant increase of the adhesion fracture energy is observed in the sample 17.2, so it can be concluded that the 2.5 nm thick Ti interlayer enhances the adhesion between copper and carbon.

COHESIVE LAW CALIBRATION

The crack length vs. penetration depth curve from figure 3 will be used as the reference to calibrate the cohesive elements for the FE model. Only the experimental results obtained for sample 17.2 (with Ti interlayer) are used as a reference because, as mentioned earlier, the data for sample 17.1 were not consistent. Figure 5 shows a comparison between interfacial crack observed in the experiments and the FE simulation results. A very good qualitative agreement between the actual crack and the simulated one can be observed.

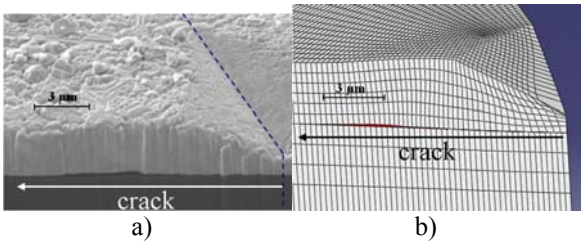

Figure 5. Cross-section view across a top indentation test: (a) SEM image of a FIB milled trench and (b) FE simulation.

A parametric study has been performed in order to calibrate the cohesive law. The parameters considered have been on one hand the fracture energy G, the initial stiffness E_i, and the peak stress σ_{max}, defining the cohesive law, and on the other hand the Cu yield stress σ_y and its hardening coefficient n, defining the plastic behaviour of the Cu film. Several simulations have been performed using as average values 2 J/m^2 for G, 200 GPa for E_i, 150 MPa for σ_{max}, 500 MPa for σ_y and 0 for n. In the case of the cohesive law parameters these values were chosen after some first tries whereas the data for Cu correspond to a 1 µm thick layer [13, 14].

The initial stiffness defines the elastic response of the cohesive elements until damage starts. It has to be big enough not to increase the compliance of the structure but too high values may lead to numerical problems. Simulations varying E_i from 200 to 400 GPa resulted in a decrease of the crack length of around half a micron. It can be concluded that the effect of this parameter is negligible for the problem studied and hence it was decided to fix its value at 200 GPa, roughly twice the elastic modulus of Cu.

Regarding G and σ_{max}, the initial calculations were performed with values of 50 J/m^2 and 500 MPa, respectively, using as reference the fracture energy calculated using ME for sample 17.2 and the elastic limit of Cu. However no cracks were observed in the simulations and thereafter values for both parameters were decreased. G was varied from 30 to 2 J/m^2 and σ_{max} from 400 to 100 MPa. Results of these simulations are shown in Table 4 and figure 6, where the crack radius at the interface for an indentation depth of 2500 nm is gathered for different values of σ_{max} and G. It is noted that snap-back convergence problems appears as σ_{max} is increased or G is decreased. It is shown that the crack increases with peak stress, but the increase is slight (around 1 µm) and saturates for peak stresses above 200 MPa. Concerning the effect of the fracture energy, as expected it is the parameter which affects the delamination to a greater extent: crack radius at the interface increases significantly as fracture energy decreases. However two regimes can be observed in the range simulated, both showing a roughly linear dependence but with different values of the slope. In

fact the ratio crack radius to fracture energy increases in an order of magnitude when G is below 10 J/m^2. For a stronger interface the plastic deformation of the Cu layer will be higher and hence a bigger amount of the energy introduced in the system will be expended in plastic deformation and will not contribute to the crack extension.

Table 4. Interfacial crack radius for different values of fracture energy and peak stress at a nanoindentation depth of 2500 nm. 'X' means simulations not completed due to convergence problems.

Crack Radius a (±0.3 μm)		G (J/m^2)				
		2	5	10	20	30
σ_{max} (MPa)	100	17.7	13.1	8.9	7.7	6.9
	150	18.3	14.2	9.7	8.3	7.4
	200	X	X	10.6	8.6	8.0
	250	X	14.9	X	8.6	8.0
	300	X	X	X	8.6	8.0
	350	X	X	X	0	0
	400	0	0	0	0	0

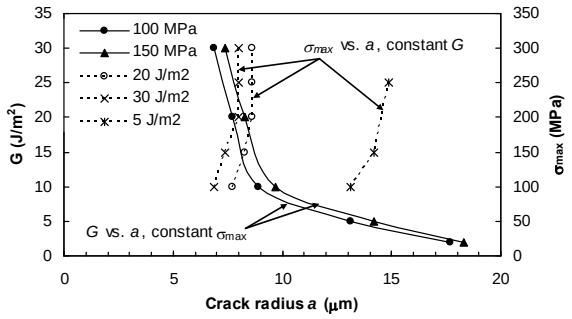

Figure 6. Effect of fracture toughness G and peak stress σ_{max} on the delamination extent (crack radius a). Solid lines curves represent G vs. a for different values of σ_{max} and dotted curves represent σ_{max} vs. a for different values of G.

To study the effect of the plastic behaviour of the Cu on the top indentation test results simulations were performed for yield strength values between 220 and 500 MPa and hardening coefficients between 0 and 0.3. The ranges were selected according to data from literature for different Cu layers [13, 14]. Figure 7 shows the effect of σ_y and n on the crack radius for indentations performed at a maximum depth of 1300 nm and on the slope of the crack radius vs. maximum penetration depth (see fig. 3). It is observed that the effect of the strain hardening coefficient is small and hence it was decided to define Cu as a perfect elasto-plastic material. Regarding the yield strength, a small influence is observed for values between 300 and 500 MPa. Taking this into account and experimental results obtained for Cu layers with different thicknesses [13], a value of 300 MPa is fixed for σ_y.

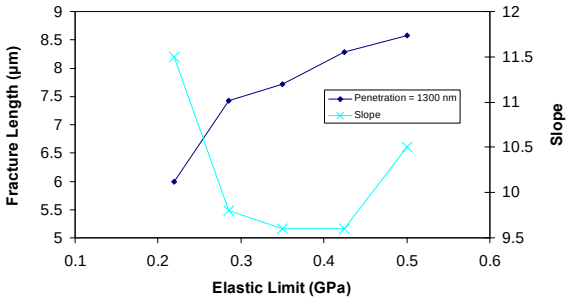

a)

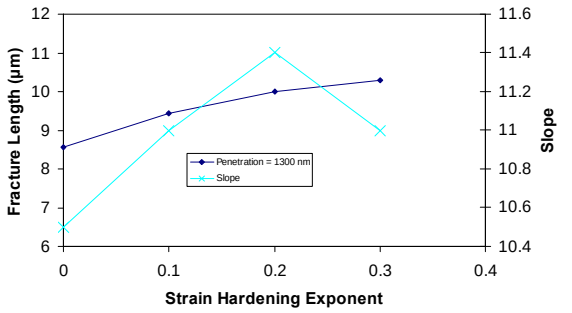

b)

Figure 7. Effect of plasticity variables in the fracture length at a penetration depth of 1.3 μm (left) and in the slope of the fracture length vs. penetration depth curve (right). a) Elastic limit and b) strain hardening exponent

Finally σ_{max} and G were varied taking into account results in table 4 with Cu defined as perfect elasto-plastic with an elastic limit of 300 MPa. Figure 8 shows the experimental and simulated crack radius vs. maximum penetration depth during a top indentation test. As can be noticed a very good agreement is found for G = 2 J/m^2 and σ_{max} = 170 MPa. A deviation from the experimental results is observed for indentation depths below 1300 nm approximately, which can be explained by the structure of the Cu layer described in the previous section.

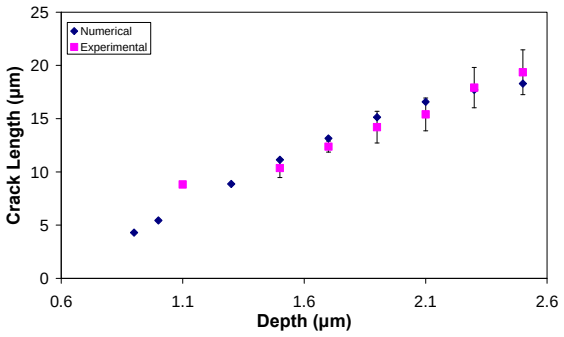

Figure 8. Experimental and simulated (σ_{max} = 150 MPa and G = 2 J/m^2) crack lengths for different indentation depths. Good agreement can be observed.

Additionally, fracture energy is 30 times lower than that calculated through ME for sample 17.2. This effect was also observed in [14], where the plasticity contribution to adhesion was calculated for a 4 point bend test.

CONCLUSIONS

It is shown that top indentation is a suitable technique to determine interfacial adhesion, even if in this work the results are limited due to the structure of the Cu layer (roughness, porosity). However it can be concluded that introducing a Ti nanometric interlayer improves adhesion between Cu and amorphous carbon.

The results from the top indentation tests, in particular the curve crack radius versus penetration depth can be used to calibrate the parameters of a cohesive law which will define adhesion between Cu and amorphous carbon. It is shown that for the system studied the adhesion is overestimated when the analytical models proposed in [2] are used. This is probably related to the plastic energy dissipated during the test and the deformation of the carbon substrate.

REFERENCES

[1] Villard, P., Calvert, L.D., "Pearsons's Handbook of Crystallographic Data", 2nd edR, *ASM International,* Materials Park, Ohio 1991.

[2] Marshall, D.B. and Evans, A.G., "Measurement of adherence of residually stressed thin-films by indentation .1. Mechanics of interface delamination", *J. Appl. Phys.*, Vol. 56, p. 2632 1984.

[3] Segurado, J., *Micromecánca computacional de materiales compuestos reforzados con partículas,* Ph.D. Thesis, Delft, Spain, 2009.

[4] Moreno, C.M., Sanchez, J.M., Ardila, L.C., Molina-Aldareguia, J.M., "Determination of residual stresses in cathodic arc coatings by means of the parallel beam glancing X-ray diffraction technique", *Thin Solid Films*, Vol. 518, p. 206, 2009.

[5] Cullity, B.D., *Elements of X-Ray Diffraction*. Addison-Wesley 2nd ed., 1978.

[6] Kriese, M.D. and Gerberich, W.W., "Quantitative adhesion measures of multilayer films: Part I. Indentation mechanics", *J. Mater. Res.*, Vol. 14, Issue 7 p. 3007, 1999.

[7] Lee, A., Clemens, B.M., Nix, W.D., "Stress induced delamination methods for the study of adhesion of Pt thin films to Si", *Acta. Mater.*, Vol. 52, p. 2081, 2004.

[8] Kese, K.O., Li Z.C., Bergman, B., "Method to account for true contact area in soda-lime glass during nanoindentation with the Berkovich tip", *Mat. Sci. Eng. A*, Vol. 404, Issue 1-2, p. 1 2005.

[9] Gong, J.H., Miao, H.Z., Peng, Z.J., "Analysis of the nanoindentation data measured with a Berkovich indenter for brittle materials: effect of the residual contact stress", *Acta Mater.* Vol. 52, Issue 3, p. 785, 2004.

[10] Matweb, "Copper, Cu; Annealed", *http://www.matweb.com*

[11] Matweb, "Vitreous Carbon", *http://www.matweb.com*

[12] Tvergaard, V. and Hutchinson, J.W., "The influence of plasticity on mixed mode interface toughness", *J. Mech. Phys. Solids*, Vol. 56, p. 2632 1984. Vol. 41, Issue 6, p. 1119, 1993.

[13] Vinci, R. P., Zielinski, E. M., Bravman, J. C., "Thermal strain and stress in copper thin films", *Thin Solid Films*, Vol. 262, Issues 1-2, p. 142, 1995.

[14] Lane M., Dauskardt, R.H., Vainchtein, A., Gao, H.J., "Plasticity contributions to interface adhesion in thin-film interconnect structures", *J. Mater. Res.*, Vol. 15, Issue 12, p. 2758, 2000.

[15] Ocaña, I., Molina-Aldareguia, J.M., Gonzalez, D., Elizalde, M.R., Sánchez, J.M., Martínez-Esnaola, J.M. Gil Sevillano, J.,Scherban, T., Pantuso, D.. Sun, B., Xu, G., Miner, B., He, J. Maiz, J. "Fracture characterisation in patterned thin-films by cross sectional nanoindentation", Acta Mater, Vol 54, p. 3453, 2006.

ACKNOWLEDGEMENTS

Financial support from the EC (Project Interface FP6 STRP 031712) and Basque Government (PhD Grant, project PI07-17) is acknowledged. Dr. Finn Giuliani is acknowledged for providing the samples. D. Marcos is grateful to the Spanish Ministry of Science and Innovation and to the European Social Fund (Torres Quevedo Programme). J. Tamayo-Ariztondo is grateful to the Basque Government for his PhD grant.